



Transactions, SMiRT-25
Charlotte, NC, USA, August 4-9, 2019
Division III

PROBABILISTIC SEISMIC SSI ANALYSIS SENSITIVITY STUDIES FOR BASE-ISOLATED NUCLEAR STRUCTURES SUBJECTED TO COHERENT AND INCOHERENT MOTIONS

Dan M. Ghiocel

Chief of Engineering, Ghiocel Predictive Technologies, Inc., NY, USA (dan.ghiocel@ghiocel-tech.com)

ABSTRACT

The paper investigates the seismic SSI effects for a base-isolated nuclear island subjected to coherent and incoherent motions. Two types of base-isolators are considered: 1) Lead-Rubber Bearing (LRB) isolators (Shimizu et al., 2015) that act efficiently in the 2D horizontal plane and 2) Base Control System (BCS) isolators (Nawrotzki et al, 2018) including a combination of spring units and high-viscosity damper (HVD) units that act efficiently in all 3D space directions. The paper also investigates the effects of motion incoherency on the structure SSI responses. Both rock and soil sites are considered. In accordance with the ASCE 4-16 standard Section 12 that requires a set of at least 30 randomized SSI inputs (at least 10 deterministic seismic inputs and 3 deterministic soil profiles), in the present study a number of 60 probabilistic simulations of the seismic input motion and the soil profile were used. The LRB isolators are modelled as hysteretic systems, while the HVD isolators are modelled as frequency-dependent dissipative systems. The SSI responses are compared in terms of structural displacements and ISRS. To perform the probabilistic nonlinear seismic SSI analyses, the ACS SASSI V4 software (Ghiocel, 2019) with Options PRO (probabilistic SSI) and NON (nonlinear structure for hysteretic isolators) was used. The paper provides important insights on the SSI effects for seismically base-isolated nuclear structures. The paper also shows the limitation of the 2D LRB isolators in comparison with the 3D HVD-based isolators.

INTRODUCTION

The application of the seismic base-isolation technology for seismic building design is one of the fundamental technologies to enhance the earthquake-proof safety of NPPs and achieve standard designs that do not depend on the seismic and soil site-specific conditions. To maintain the integrity of reactor buildings against severe earthquakes, which might occur in future in many possible places, the base-isolation systems are considered be highly effective engineering approaches.

This paper investigates through a series of sensitivity studies: 1) the effects of the base-isolation against no isolation for both rock sites and soil sites, 2) the effects of motion incoherency, 3) the use of probabilistic SSI vs. deterministic SSI, 4) the effects of using the 3D HVD-based isolators (Nawrotzki et al, 2018, Kostarev et al., 2018) against the traditional 2D LRB isolators (Shimizu et al., 2015).

PRELIMINARY DETERMINISTIC SSI STUDIES

A typical reactor building complex (RBC) is considered for the base-isolation studies. The preliminary studies performed in 2015 compared “With isolators” and “Without isolators” cases for rock sites and soil sites, including both coherent and incoherent motion inputs. Only the LRB isolators were considered. The seismic SSI analysis study results were communicated at few nuclear meetings, but not included so far in any technical paper. This section includes a brief summary of the key findings of the preliminary studies completed in 2015.

Figure 1 shows the investigated base-isolated RBC system. A detailed FE model with about 40,000 nodes was used to model the RBC structural system. The bottom basemat was considered with realistic concrete elastic stiffness, not as a rigid slab. For base-isolation a number of 309 LRB isolators with a 1.6m diameter manufactured in Japan were considered (Shimizu et al., 2015). The LRB isolators were modeled using nonlinear hysteretic springs elements (using ACS SASSI Option NON). To include the LRB nonlinear hysteretic behavior an iterative equivalent-linearization procedure was used (see left-side of Figure 1). The LRB isolators are placed between a top basemat and a bottom basemat with a thicknesses of 15 ft.

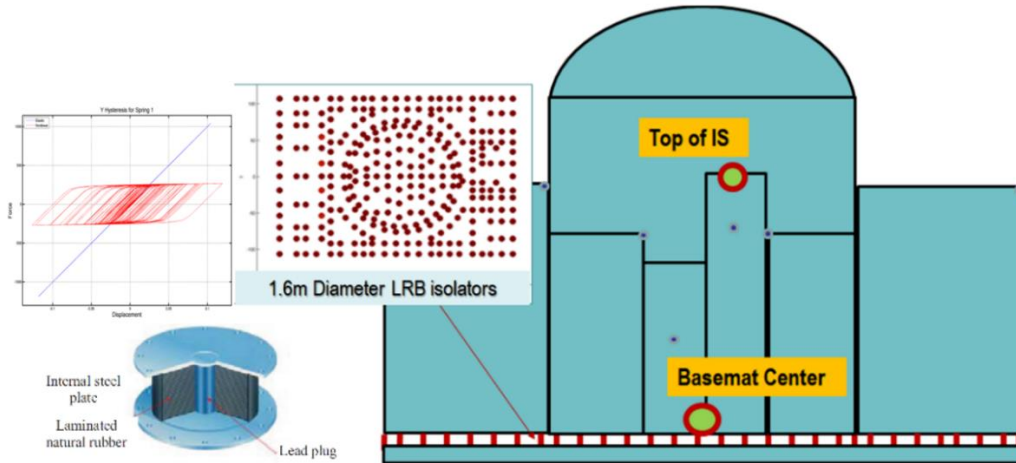


Figure 1 Base-Isolated RB Complex System with 1.6m Diameter LRB Isolators

The initial preliminary studies were deterministic coherent SSI analyses to investigate the effects of the site soil condition on the efficiency of the base-isolation system. The rock site layering was idealized by a uniform rock formation with a $V_s = 6,000$ fps, while the soil site layering was idealized by a uniform soil with $V_s = 1,000$ fps. The seismic input was defined by RG1.60 spectrum-compatible acceleration motion input in all 3D space directions. The maximum ground acceleration was 0.3g in the horizontal and vertical directions.

Figures 2 and 3 show the ISRS computed at the center of the top basemat (see location in Figure 1) for the rock site and the soil site for the “With isolators” (red lines) and “Without isolators” (blue lines). Figure 2 shows the ISRS in X-longitudinal direction, and Figure 3 shows the ISRS in the Z-vertical direction. The left plots are for the rock site and the right plots are for the soil site.

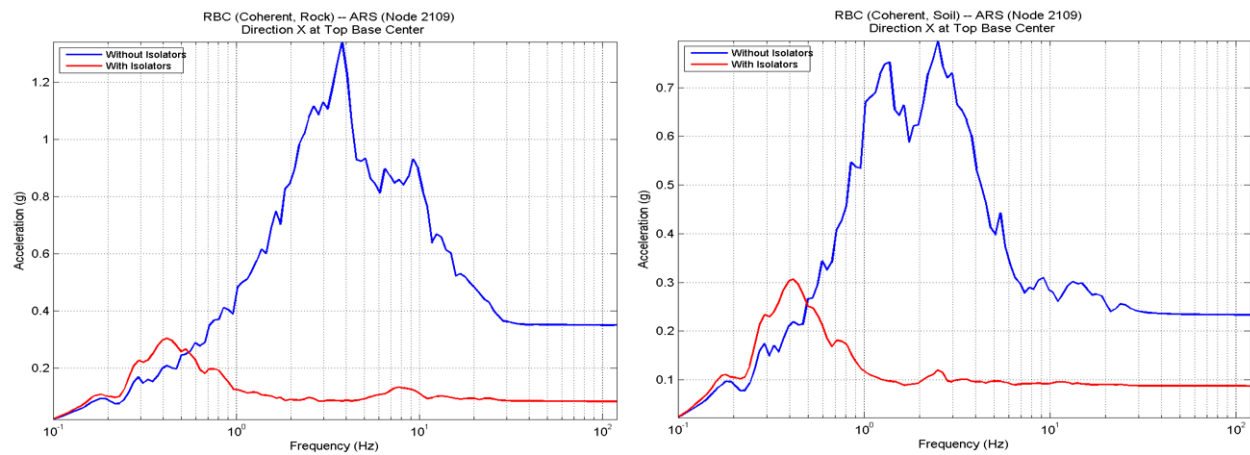


Figure 2 X-Direction ISRS for Rock Site (left) and Soil Site (right) for with and without LRB isolators

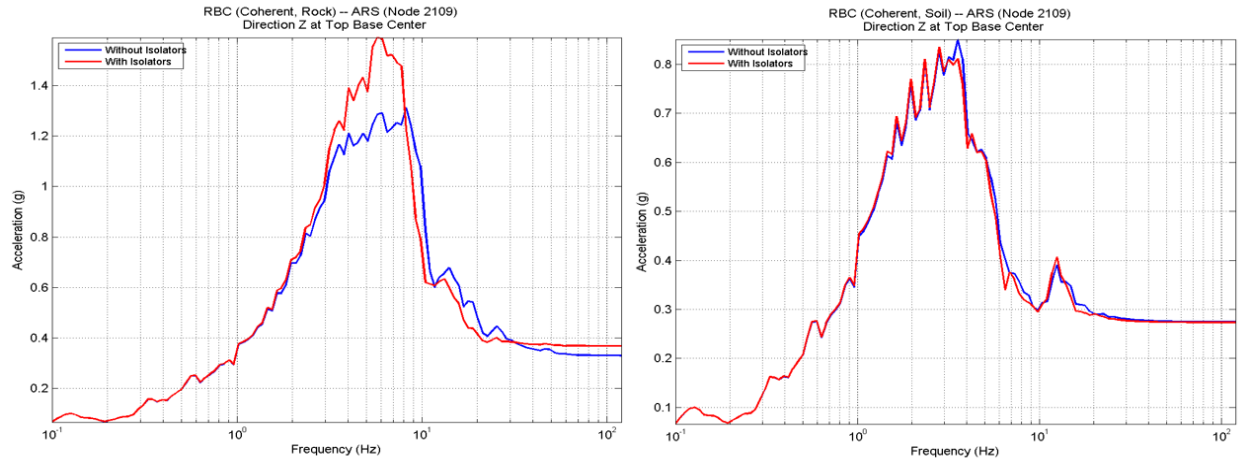


Figure 3 Z-Direction ISRS for Rock Site (left) and Soil Site (right) for with and without LRB isolators

It should be noted from Figure 2 that the LRB base-isolation reduces largely the ISRS amplitudes for both the rock site and the soil site. The ISRS peak reduction is about 4 times for rock and only 2.5 times for soil. Therefore, the base-isolation is most effective for rock sites. This is a result is based on the fact that the base-isolation system shifts the RB complex dominant vibration frequency to very low frequencies, practically cancelling the effects of the SSI radiation damping that manifests at higher frequencies. The SSI damping benefit is lost, but the base-isolation benefit is still large as shown in Figure 2 for the soil site.

Figure 3 shows the effects of the LRB base-isolation for the vertical ISRS, which are is either none or almost none. Moreover, sometimes could even produce small amplifications of the ISRS spectral peaks. This lack of effectiveness of LRB isolators for vertical motions appears to be a serious practical limitation of the LRB base-isolation technology for applications to the future advanced nuclear reactors.

Figure 4 provides an additional insight for the base-isolation effects for rock and soil sites. The RBC base-isolation basically vanishes the beneficial SSI radiation damping effects, but it does not cancel the shift in dominant SSI mode frequencies that are related to the soil foundation stiffness. The ISRS peaks for the soil sites shift to significantly lower frequencies with no reduction in the ISRS peak amplitudes. These ISRS results indicate that the SSI effects are very important for the base-isolated structures. It should be also noted that in the low frequency range, below 1 Hz, the global sliding motion of the base-isolated structure is the same for the rock site and the soil site.

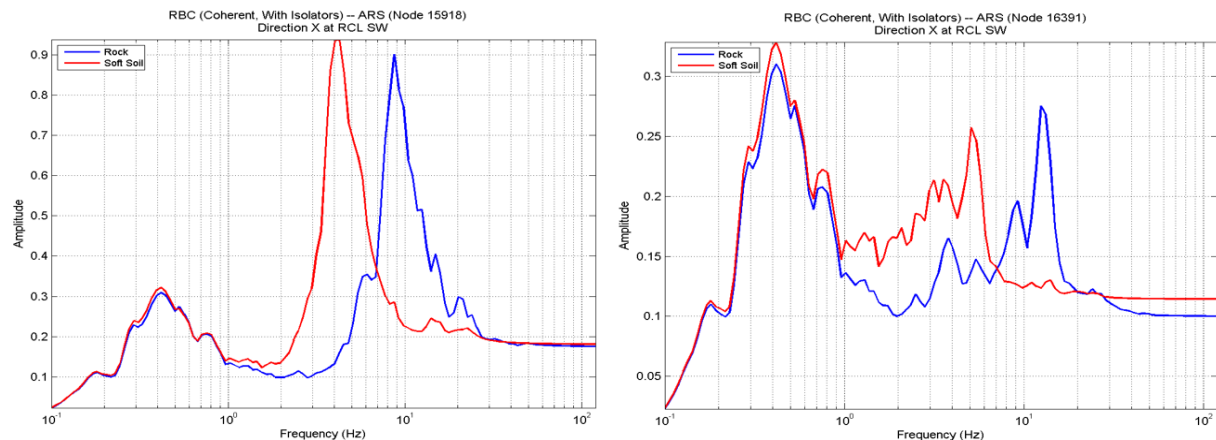


Figure 4 X-Direction ISRS at Higher Elevations in RBC for Rock Site (blue line) and Soil Site (red line)

An important influential factor that could largely affect the ISRS for base-isolated RBC is the motion incoherency. The incoherent motions produce differential soil motions under the bottom basemat that partially transmit as nonuniform seismic loads on the isolators. These incoherent differential soil motions excite some structural modes that are not excited by the coherent motion, since the coherent motion produces no soil differential motions.

For the comparative coherent vs. incoherent SSI analysis study, a uniform soil deposit with a V_s of 2,000 fps was considered. The incoherent motion was defined based on the Abrahamson coherence function for soil sites (Abrahamson, 2007). Additionally, an apparent traveling wave velocity of 6,000 fps was included to simulate the wave passage effects in the X-longitudinal direction. For the incoherent SSI analysis, the rigorous stochastic simulation approach (with no phase adjustment) based on the Monte Carlo wavefield simulations was used. Several incoherent seismic wavefields were simulated.

Figure 5 shows the large motion incoherency effects on ISRS at the top of the RBC Internal Structure for X and Z directions. Five incoherent simulated results are compared with coherent results. Motion incoherency amplifies the horizontal ISRS peak by several times (direction for which base-isolation is effective), while reducing the vertical ISRS peak (direction for which base-isolation is not effective).

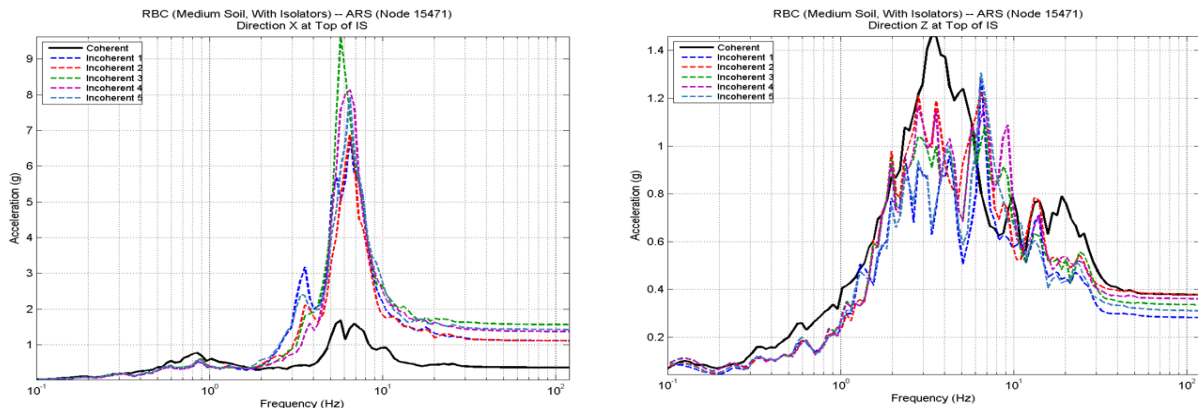


Figure 5 Incoherent vs. Coherent ISRS at Top of RBC Internal Structure in X (left) and Z (right) Directions

Another important practical aspect is that the motion incoherency amplifies the differential displacements within RBC. Figure 6 shows the ratios between incoherent and coherent displacements in various locations at different elevations with respect to the center of the top basemat. It should be noted that the incoherent relative displacements are up to 3 times larger in horizontal direction and 6 times larger in vertical direction. Motion incoherency also severely increases the axial forces in the LRB isolators (not shown herein).

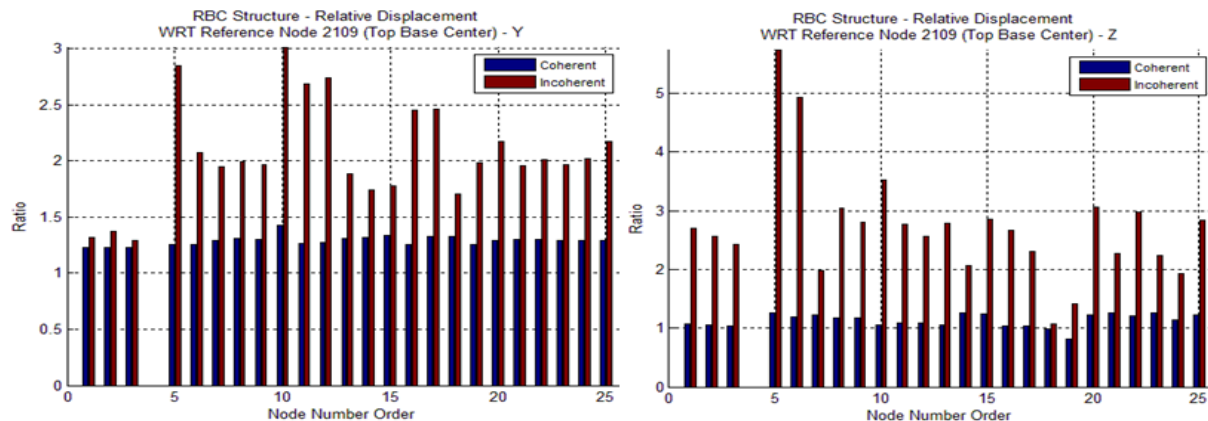


Figure 6 Incoherent vs. Coherent Relative Displacements Within RBC for X (left) and Z (right) Directions

PROBABILISTIC SSI STUDIES

New research studies were performed in early 2019 for the same seismically base-isolated RBC building shown in Figure 1. The probabilistic seismic SSI analysis is based on the ASCE 4-16 standard recommendations in Sections 2, 5 and 12. The SSI input is defined based on the site-specific conditions.

The site-specific seismic input is defined by a probabilistic outcrop UHRS at the depth of 200 ft where the bedrock is located. Then, using the probabilistic UHRS, a set of 60 probabilistic simulations with randomized spectral content are considered for the nonlinear PSRA. The probabilistic UHRS simulation follows the Method 2 procedure in the ASCE 4-16 Section 5.5. The 60 simulations are shown in Figure 7. The black lines are the 60 simulations, while the green lines and blue lines are the target and computed probabilistic URHS curves for the mean and the mean minus/plus standard deviation. The probabilistic UHRS amplitude variations were modelled assuming a lognormal distribution with a c.o.v of 28% and a correlation length of 10 Hz, in accordance with the guidelines for applying Method 2. Figures 8 and 9 show the 60 simulations for the low-strain Vs and D soil profiles, and the nonlinear soil material constitutive curves used for the shear modulus and damping as function of the soil shear strain. The Vs profile c.o.v. is variable with depth from 10% to 20% and its correlation length varies from 10 ft and 40 ft.

It should be noted that in this research study does not follow in detail the regulatory requirements for performing the probabilistic site response analysis (PSRA) which is performed as the basis for the probabilistic SSI analysis (PSSIA). The departure from the regulatory requirements for PSRA is generated by the fact that the bedrock UHRS input spectral content was randomized before performing the nonlinear site response analyses. The applied PSRA procedure mimics in a simpler way the bedrock UHRS probabilistic-based deaggregation process with the use of the Approach 3 recommended by the ASCE 4-16 and USNRC RG1.208.

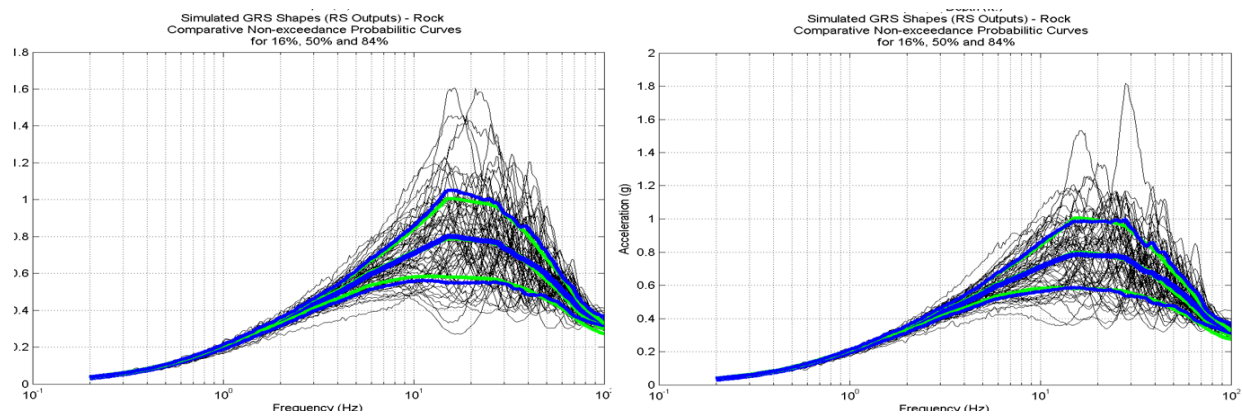


Figure 7 Simulated Bedrock UHRS at 200 ft Depth in Horizontal (left) and Vertical (right) Directions

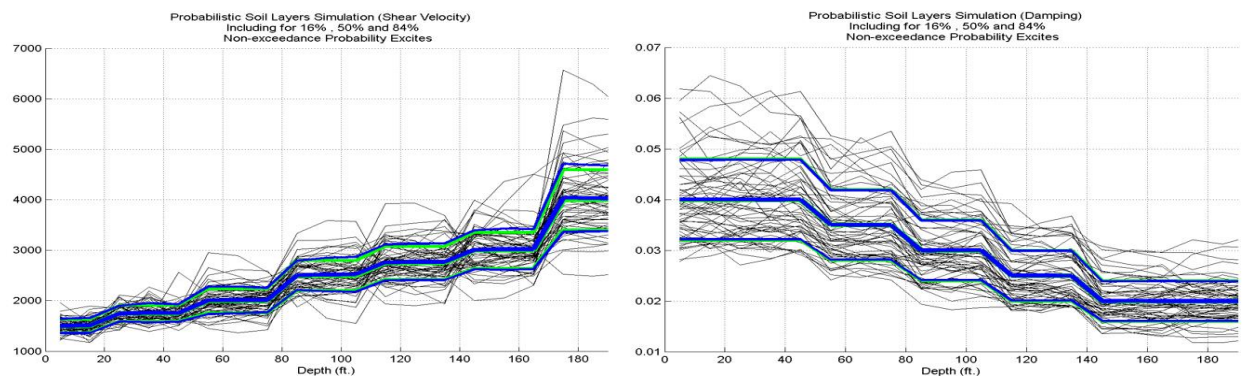


Figure 8 Simulated Low-Strain Vs (left) and D (right) Soil Profiles

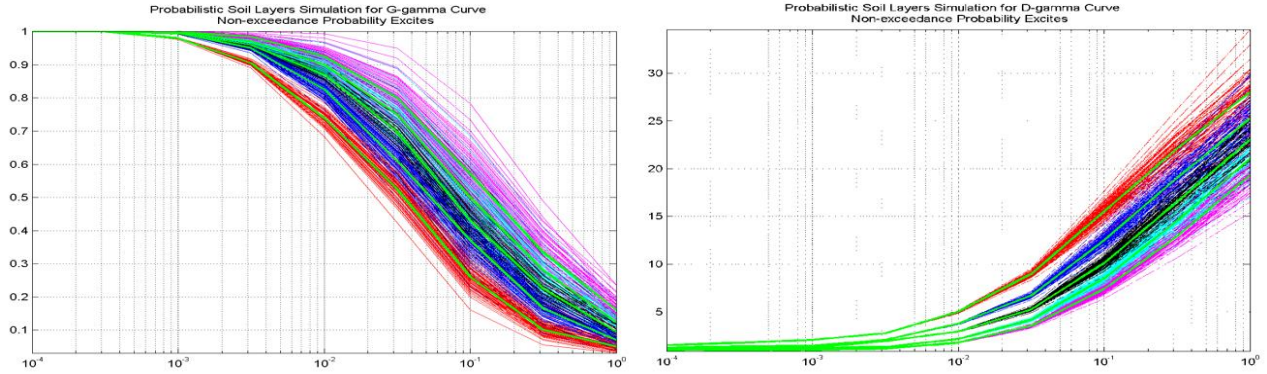


Figure 9 Simulated Soil Material Curves for Shear Modulus and Damping Curves (at 5 Depths)

The 60 simulated soil surface UHRS are shown in Figure 10 for horizontal and the vertical directions. The soil surface UHRS were simulated based the 1D nonlinear motion convolutions based on the assumption of the vertically propagation of body waves (using SHAKE methodology).

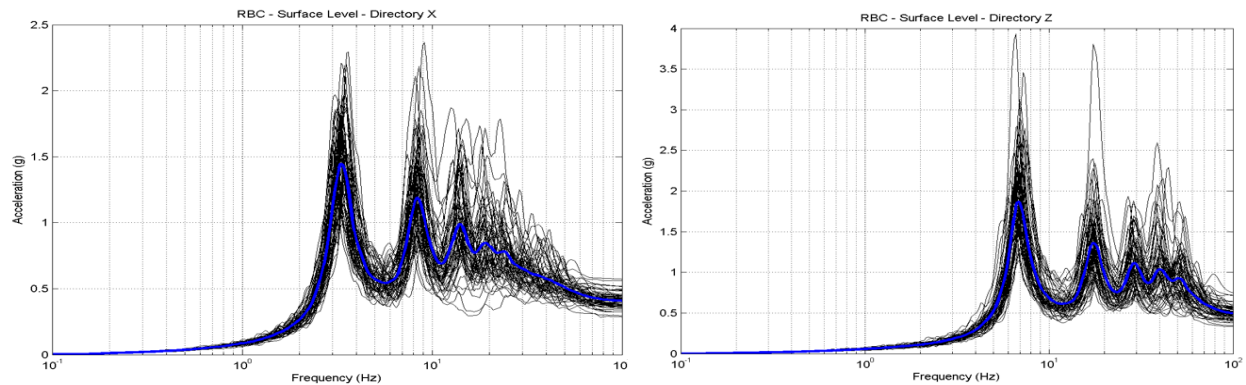


Figure 10 Surface Soil UHRS Simulations and Mean Value (blue) in Horizontal and Vertical Directions

The Figure 11 the left-side plot shows the low-strain and iterated V_s probabilistic soil profiles for the mean and the mean minus/plus standard deviation. The low-strain V_s profiles are plotted with green lines and the iterated V_s profiles are plotted with blue lines. On the right-side plot it is shown the deterministic LB, BE/mean and UB V_s soil profiles defined based on the V_s simulated profiles for the mean and the mean minus/plus standard deviation values. The right-side plot shows the ratio between the V_s of the deterministic LB, BE/mean and UB soil profiles divided by the V_s of BE/mean soil profile.

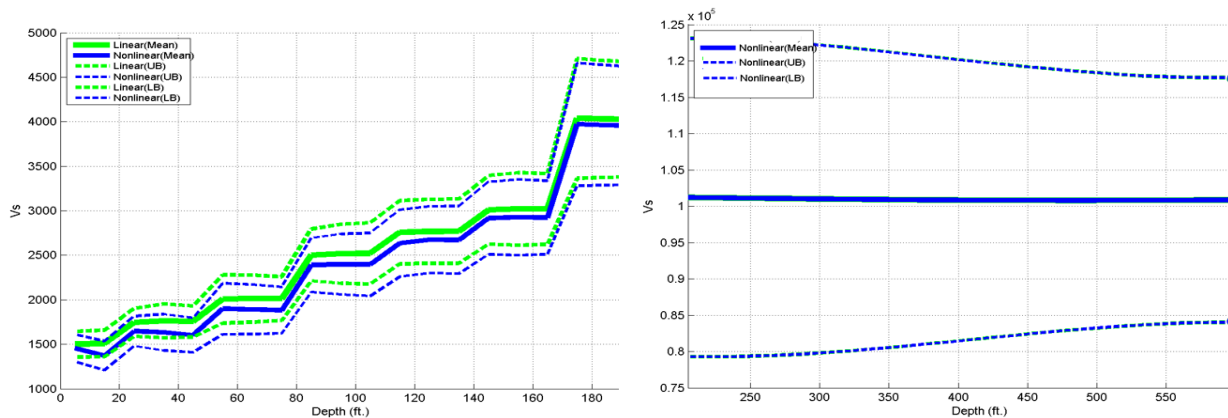


Figure 11 Statistical V_s Soil Profiles (left) and Deterministic Ratios for LB, BE, UB V_s and Mean V_s

Figures 12, 13 and 14 show comparative probabilistic vs. deterministic SSI results for the base-isolated RBC using the 1.6m diameter LRB isolators (Shimizu et al., 2015). Figure 12 shows for the 60 simulated ISRS (black), probabilistic mean ISRS (blue) and deterministic LB-soil ISRS, BE-soil ISRS and UB-soil ISRS (red) for the center of the top concrete basemat. Deterministic SSI results were obtained for five sets of the spectrum-compatible acceleration motions simulated in X, Y and Z directions. Seismic input motions were assumed to be coherent motions. It should be noted that in the horizontal direction the probabilistic mean ISRS is well above the envelope of the three deterministic ISRS. This indicates that the deterministic SSI provides unconservative ISRS for the horizontal direction. However, for the vertical direction for which the LRB isolators are not effective, the envelope of deterministic ISRS is larger than the probabilistic mean ISRS.

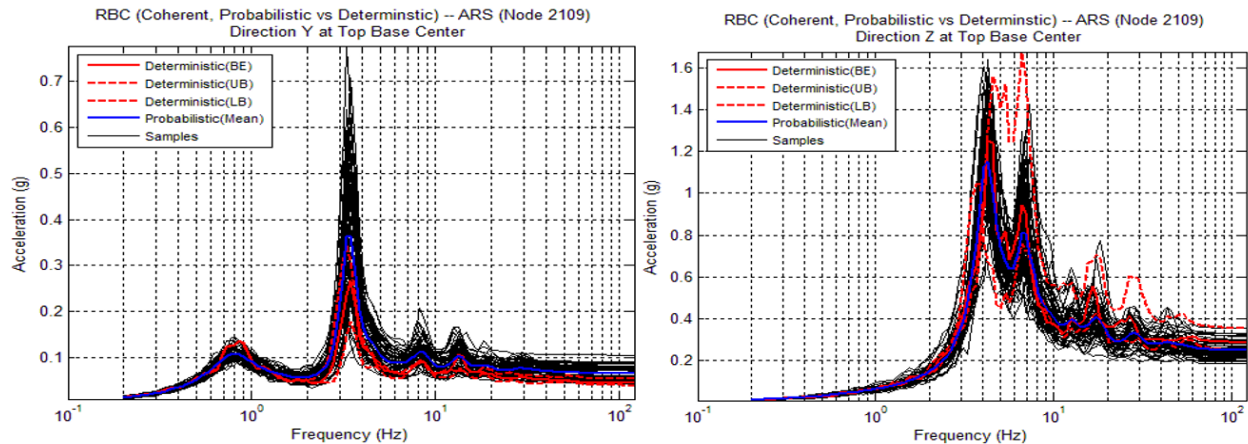


Figure 12 Simulated, Probabilistic Mean and Deterministic Coherent ISRS for Y (left) and Z (left) Directions at the Top Basemat Center

Figures 13 and 14 show the effect of the motion incoherency on the ISRS by comparing the probabilistic mean and 80% NEP ISRS for coherent (blue) and incoherent (green) motion inputs against the envelope of the three deterministic coherent ISRS computed for the LB, BE and UB soils (red). Figure 13 includes the ISRS for the center of top basemat in Y and Z directions. Similarly, Figure 14 includes the ISRS for the top of the RBC internal structure in Y and Z directions. Both figures indicate that for the horizontal direction, the probabilistic 80% NEP *coherent* ISRS are much larger by 60-80% than the envelope of the three deterministic *coherent* ISRS. For the vertical direction, the deterministic ISRS are significantly larger than the probabilistic 80% NEP *coherent* ISRS.

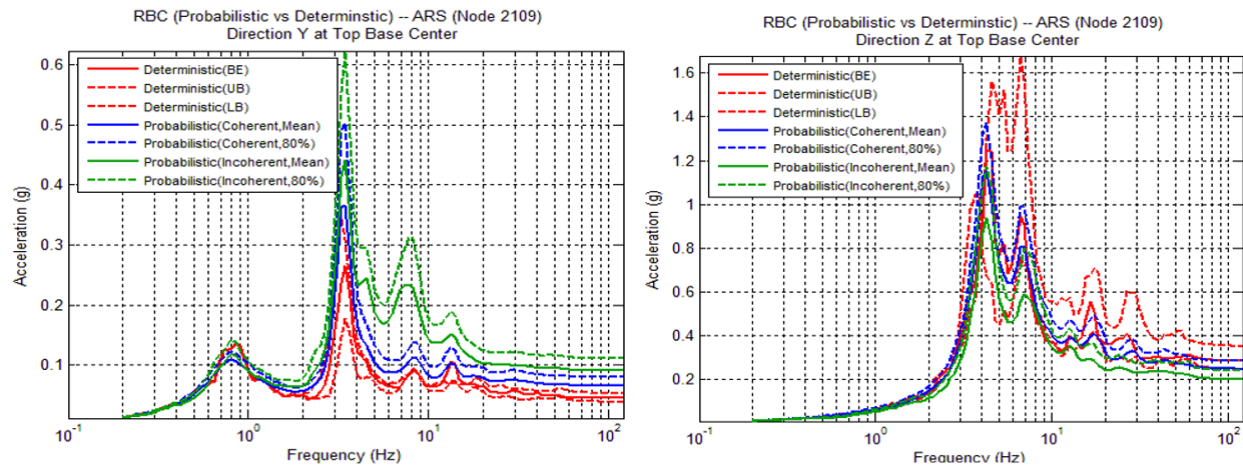


Figure 13 Probabilistic Mean and 80% NEP Coherent ISRS (blue) and Incoherent ISRS (green) vs. Deterministic Coherent ISRS (red) in Y (left) and Z (right) Direction at the Top Basemat Center

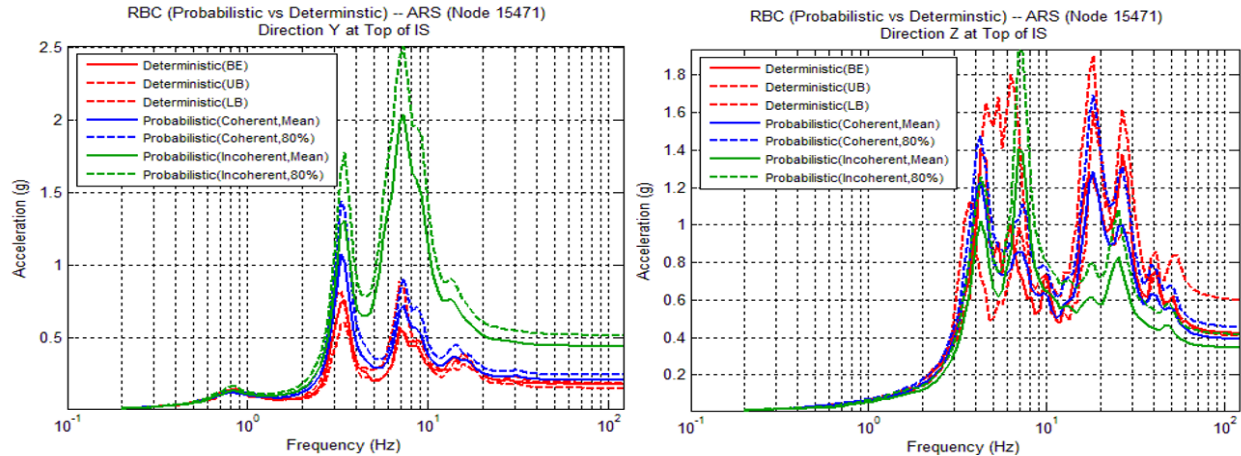


Figure 14 Probabilistic Mean and 80% NEP Coherent ISRS (blue) and Incoherent ISRS (green) vs. Deterministic Coherent ISRS (red) in Y (left) and Z (right) Direction at the Top of Internal Structure

The most important result in Figures 13 and 14 is the large detrimental effect of the motion incoherency on the horizontal ISRS computed for the base-isolated RBC using the LRB isolators. In the horizontal direction, the probabilistic 80% NEP *incoherent* ISRS are much larger, up to 300%, than the probabilistic 80% *coherent* ISRS and the deterministic *coherent* envelope ISRS. In contrast, in the vertical direction, the deterministic envelope ISRS are the largest, except for situations when the incoherency excites some Z coupled responses for narrow frequency bands as shown in Figure 14.

An important goal of the 2019 studies has been also to compare SSI responses of the base-isolated RBC using the LRB isolators and BCS/HVD isolators, respectively. For this study, the GERB BCS isolators (Nawrotzki et al, 2018) have been considered. The GERB BCS isolators consists of the combination of spring units with high-viscous damper units as illustrated in Figure 15.

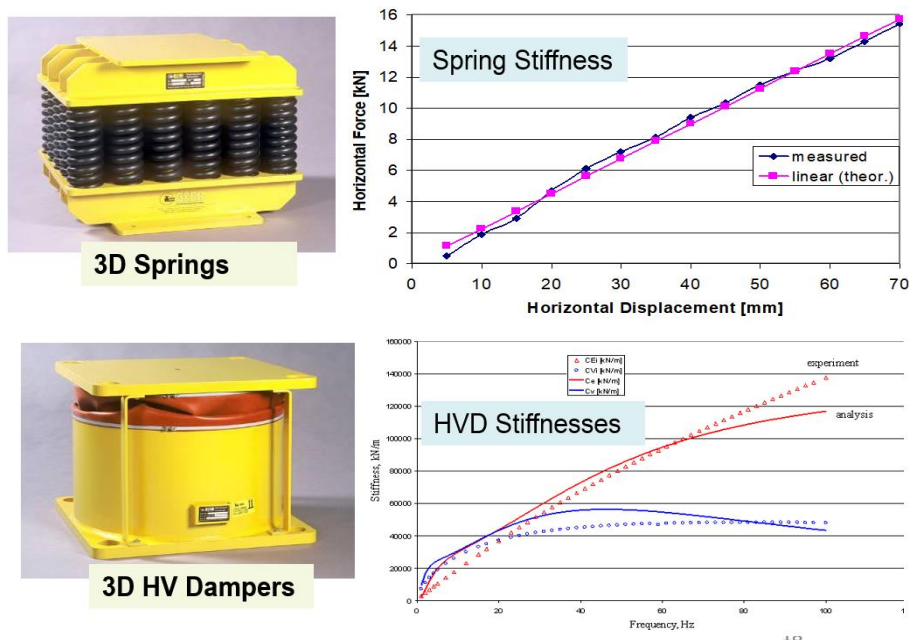


Figure 15 BCS Isolators Composed by Spring Units and HVD Units (Kostarev et al., 2018)

The combination of the spring units and the HVD units can be optimized to largely reduce the seismic SSI responses of the base-isolated structures (Kostarev et al., 2018). The number of spring units is controlled

by the vertical stiffness static capacity of the unit for vertical loads. However, the number of HVD units is variable and can be increased to produce more damping. The fact that the horizontal sizes of the BCS units are smaller than the 1.6m diameter LRB size, provides the opportunity to include more units and produces a smoother more uniform variation of the seismic and gravity loads on these units.

Figure 16 shows the ACS SASSI implementation of the frequency-dependent 3-node HVD elements based on the 4-parameter Maxwell that include two parallel 2-parameter chains as shown. The analysts have only to input the four parameters K_1 , K_2 and B_1 , B_2 , each with two different values for horizontal and vertical directions. These four parameters are frequency-dependent parameters, as described in Figure 15 for the HVD elastic and the loss stiffnesses (Kostarev et al., 2018).

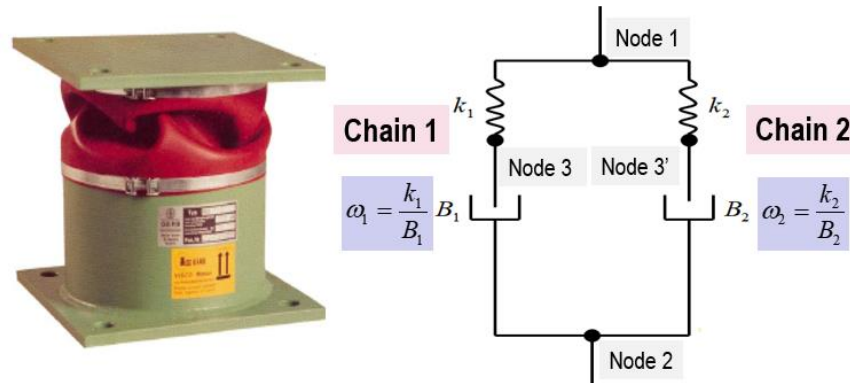


Figure 16 The HVD Unit Mathematical Modelling by 4-Parameter Maxwell Model (with Two Chains)

Since the Spring unit vertical force capacities are lower than the 1.6m diameter LRB capacities, a larger number of units were considered. Sensitivity studies were performed for different number of Spring and HVD units. The number of HVD units was varied between 309 and 618 units for getting an optimal overall SSI response. Comparative results are shown for a number of 618 HVD units.

Figures 17 and 18 show comparative probabilistic mean ISRS for “Without isolators” (blue), “HVD isolators” (red) and “LRB isolators” (green) at two critical locations within the RBC building, specifically at the top basemat center and the top of internal structure. The figures include computed ISRS for Y and Z directions for both coherent and incoherent inputs. The coherent and incoherent ISRS are plotted with the solid lines and the dashed lines, respectively.

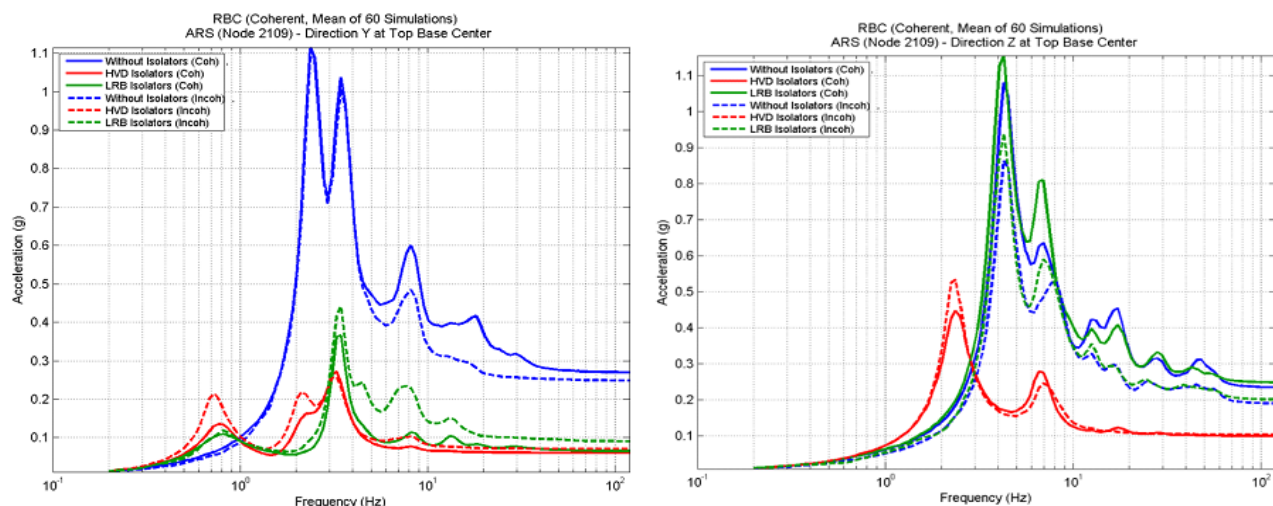


Figure 17 Comparative Coherent (solid) and Incoherent (dashed) ISRS at Basemat Center

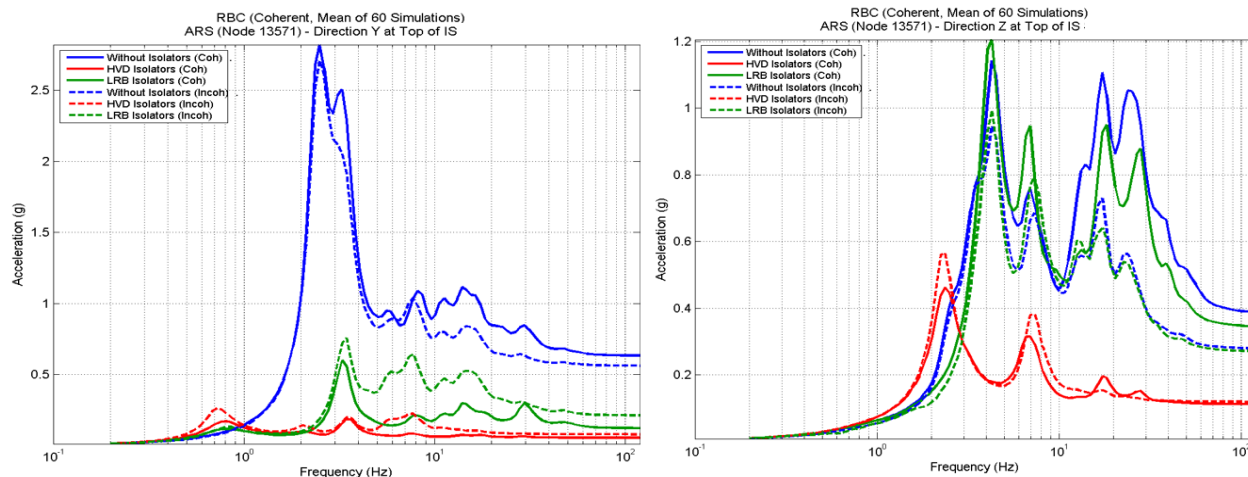


Figure 18 Comparative Coherent (solid) and Incoherent (dashed) ISRS at Top of Internal Structure

The motion incoherency effects on ISRS are slightly favourable for the RBC without base-isolation and severely unfavourable for the RBC with base-isolation, as noticed in the previous section. The incoherency effects are drastic especially for the horizontal directions. For the vertical direction, for which the “LRB isolators” are not effective, the motion incoherency effects are smaller similar to the “Without isolators” case. Figures 17 and 18 also shows that the use of the GERB BCS with the 3D HVD isolators is more effective than the 2D LRB isolators. The ISRS reductions for the “HVD isolators” are large in both the horizontal and vertical directions. The key aspect for the practical applications is that the “HVD isolators” are highly effective in the vertical direction for which the “LRB isolators” are totally ineffective.

CONCLUDING REMARKS

The paper provides a variety of comparative SSI results for the base-isolated nuclear RB complex using LRB isolators and BCS/HVD isolators. The main conclusions are that i) the RB complex base-isolation is highly effective for both the rock and soil sites, ii) the motion incoherency largely amplifies the horizontal ISRS and relative displacements within the RB complex, and iii) the 3D BCS/HVD isolators are more effective than the 2D LRB isolators especially for the vertical motions.

REFERENCES

- Abrahamson, N. (2007). “Effects of Spatial Incoherence on Seismic Ground Motions”, *Electric Power Research Institute Report No. TR-1015110*, Palo Alto, CA and US Department of Energy, Germantown, MD, December 20
- Ghiocel Predictive Technologies, Inc. (2019). “ACS SASSI - An Advanced Computational Software for 3D Dynamic Analyses Including SSI Effects”, *ACS SASSI Version 4 User Manuals, Revision 0*, Rochester, New York
- Kostarev et al. (2018).” Seismic Dynamic Analysis, Optimization, Testing and Probabilistic Safety Assessment of an Innovative 3D Seismic Base Isolation System for Important Structures”, *TINCE 2018*, France, Paris-Saclay, August 29-31
- Nawrotzki et al. (2018).” 3-D Base Control Systems for the Seismic Protection of Structures in a NPP”, *TINCE 2018*, France, Paris-Saclay, August 29-31
- Shimizu et al. (2015). “Development of Evaluation Method for Seismic Isolation Systems of Nuclear Power Facilities-A Proposal for Base-Isolated Design Methodology to Install in NPP Facilities”, *SMiRT-23, Division V, Paper 119*, Manchester, United Kingdom, August 10-14